Continuous flow synthesis of small silver nanoparticles involving hydrogen as the reducing agent†

Karel J. Hartlieb,[a,b,c] Martin Saunders,[b] Roshan J. J. Jachuck[c] and Colin L. Raston*[a]

Received 12th January 2010, Accepted 24th February 2010
First published as an Advance Article on the web 14th April 2010
DOI: 10.1039/c000708k

Two narrow-channel reactor designs have been developed and used in conjunction with gas–liquid segmented flow in order to intensify reactions and to effect synthesis under continuous flow conditions, incorporating single pass and recirculating capability, under high pressure and temperature. Silver nanoparticles approximately 3–5 nm in diameter are accessible with the average size depending on the reaction temperature and polyphosphate concentration, with smaller and more monodisperse nanoparticles produced at low polyphosphate concentrations and low temperatures. The use of continuous flow conditions leads to the possibility of simple scale-up to commercial production.

Introduction

The synthesis of noble metal nanoparticles has attracted much interest because of the unique properties these nanoscale materials exhibit which can translate into exciting applications.[1] Achieving control over the size and shape of such nanoparticles is important in optimising their properties, with increasingly more importance placed on methods that can easily be adapted and reproduced from a laboratory scale to a commercial production level. Additionally, there is also a need to produce nanomaterials using sustainable methods, incorporating green chemistry alternatives into the science at its inception. The most widely used green chemistry method for the production of nanomaterials is the Turkevich method for the synthesis of gold nanoparticles, which involves the use of sodium citrate as a reductant and stabiliser. Here the final size of the nanoparticles depends on the gold : citrate ratio, solution pH, and the presence of other species, such as tannic acid or additional stabilisers.[2-4]

Analogous reactions with silver (the Lee–Meisel method) produce an inferior colloidal product, and other reductants such as ascorbic acid and glucose have been used.[5-7] It is difficult, however, to produce silver nanoparticles with an average diameter of less than 5 nm using these methods, and it is the lower limit for generating spheroidal nanoparticles using continuous flow spinning disc processing (see below).[8] Recently, we reported the synthesis of very small, 2–3 nm silver nanoparticles, using hydrogen gas as a reductant in the presence of phosphonated calixarenes.[9] Phosphonated calixarenes act as a template to which silver cations can bind in order for the reduction reaction with hydrogen to take place. Even though the reduction potential of $Ag^+ + e^- \rightarrow Ag^0$ is 0.799 V, hydrogen cannot be used to reduce silver. This is because the aforementioned reduction half-equation applies to an electrochemical system where there is sufficient silver present upon which newly formed Ag^0 can nucleate, *i.e.*, $Ag^+ + Ag_n + e^- \rightarrow Ag_{n+1}$ (where $n = \infty$). The reduction potential for a single Ag^+ cation to be reduced to a free Ag^0 in solution is –1.8 V,[10-12] but it is known that if Ag^+ is bound to a template material the reduction reaction with hydrogen is favourable. Other polyelectrolyte templates also exist, involving the use of poly(acrylic acid) and sodium polyphosphate and hydrogen gas as the reducing agent for Ag^+.[10,11,13] Silver nanoclusters form in the presence of poly(acrylic acid), and 30–50 nm silver nanoparticles are formed in the presence of sodium polyphosphate. Interestingly the synthesis of silver nanoparticles with hydrogen is also possible in the absence of a surfactant, using silver(I) oxide as a precursor.[7,14,15]

Here we report methods for producing 3–5 nm diameter silver nanoparticles, using both batch and continuous flow process intensification methodologies, which avoids the use of harmful reducing agents, such as sodium borohydride, that are typically used to access such small particles. Process intensification is a production strategy aimed at increasing mass and heat transfer rates by orders of magnitude over conventional batch methods. Process intensification by means of a spinning disc processor has previously been reported for the synthesis of silver nanoparticles.[8] In this work we report the use of a narrow-channel reactor (NCR) as a process intensification module for the production of nanoparticles of silver. Similar modules have recently been used for the continuous production of biodiesel and the oxidation of benzyl alcohol to benzaldehyde,[16,17] as well as the synthesis of nano- and micron-sized particles.[18-21] The use of NCR is similar to microfluidic synthesis, albeit with a larger diameter channel. Synthesis under a continuous flow

[a]*Centre for Strategic Nano-Fabrication, The University of Western Australia, 35 Stirling Highway, Crawley, WA, 6009, Australia. E-mail: colin.raston@uwa.edu.au; Fax: (618) 64881005; Tel: (618) 64883045*
[b]*Centre for Microscopy, Characterisation and Analysis, The University of Western Australia, 35 Stirling Highway, Crawley, WA, 6009, Australia*
[c]*Process Intensification and Clean Technology (PICT) Group, Department of Chemical & Biomolecular Engineering, Clarkson University, Potsdam, NY, 13699, USA. E-mail: rjachuck@Clarkson.edu*
† Electronic supplementary information (ESI) available: Evolution of optical properties with time, comparison of absorption intensity for batch and recirculating NCR experiments, comparison of reagent feed volume for recirculating NCR experiments, and TEM image for high NaTPP for recirculating NCR experiments. See DOI: 10.1039/c000708k

regime lends itself to easy scale-up to commercial production quantities, simply by operating the reactor for a longer period or by using multiple reactors operating in parallel to create a so-called monolith reactor. The use of a process intensification methodology also overcomes problems prevalent in scaling up batch reactions, in particular a decreased surface area to volume ratio with increasing vessel volume, leading to poorer mixing and consequently a lower quality colloidal product.

Experimental

Two narrow-channel reactors were constructed, a recirculating reactor and a pressurised, high-temperature, single-pass reactor, Fig. 1. A solution containing 1 mM silver nitrate and the desired concentration of sodium polyphosphate (NaPP, chain length 12–13 phosphate units) or sodium tripolyphosphate (NaTPP) at pH = 9 were prepared and heated to a specified temperature. For process intensification experiments the solution was then pumped into a narrow-channel reactor whereupon the solution was mixed with hydrogen gas at a T-mixer, generating segmented gas–liquid flow (also known as bubble-train, slug, or Taylor flow). Batch reactions were carried out by stirring the solution using a magnetic stirrer and bubbling hydrogen into the solution at ambient pressure.

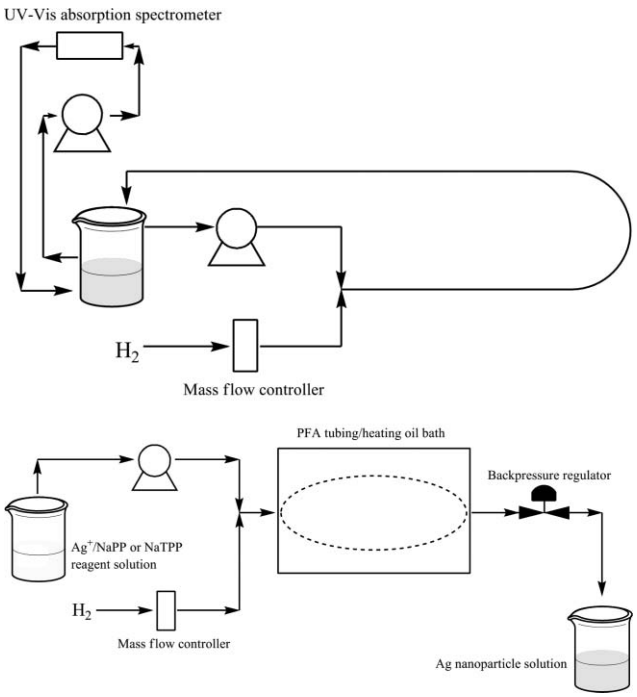

Fig. 1 Top: recirculating NCR design. Bottom: pressurised, high-temperature, single-pass NCR design.

The recirculating narrow channel reactor was designed as a tube-in-tube reactor constructed with PFA tubing, with recirculating heating fluid flowing through the outer tubing and the gas–liquid reaction mixture flowing through the inner tubing. The length of the inner tubing was set to 2.69 m (106 in) with an internal diameter of 1.59 mm (1/16 in). The solution was pumped into the reactor with a gear pump and the hydrogen flow rate was controlled with a mass flow controller. The optical properties of the recirculating solution were continuously monitored by pumping the reagent feed solution through a VWR medium-flow mini-peristaltic pump to a 1 cm path length, Starna quartz flow cell cuvette, and the UV-Vis absorption spectrum was acquired by an OceanOptics USB4000-UV-Vis spectrometer with a USB-DT deuterium–tungsten halogen light source.

The pressurised, high-temperature, single-pass reactor consisted of 30.48 m (100 ft) of PFA tubing with an internal diameter of 1.59 mm, constructed from four 7.62 m (25 ft) lengths connected with union fittings. The solution and hydrogen were again mixed with a T-mixer in creating segmented flow, and a back-pressure regulator was fitted to the output of the reactor. The tubing was placed in an Thermo Scientific DC30-W19/B open bath circulator filled with Dow Corning 200 50 cs heating fluid, and the reagent solution was pumped into the reactor using a Chrom Tech P100 HPLC prep pump. The hydrogen flow rate was controlled with a mass flow controller. The optical properties were measured post-reaction using the previously mentioned spectrometer without the continuous analysis setup. All tube fittings and adapters were purchased from Swagelok and all tubing was purchased from Cole-Parmer.

Particle size characterisation was carried out using a JEOL 2100 transmission electron microscope (TEM) with a LaB_6 filament at an operating voltage of 200 kV, or a JEOL 3000F TEM operating at 300 kV, and measuring at least 1000 particles to obtain an average diameter and standard deviation.

Results and discussion

Influence of flow parameters, temperature, and polyphosphate concentration for the recirculating NCR

Initial experiments were undertaken using a recirculating narrow-channel reactor with a reagent feed volume of 200 mL heated to 70 °C, in the presence of 0.05% w/v NaPP. Various liquid and gas flow rates were examined, and the corresponding optical properties of the recirculating solution were monitored over time in order to optimise reaction conditions. The intensity of the absorption spectrum after a specific time shows that the flow conditions using 10 mL min^{-1} liquid and 5 mL min^{-1} hydrogen resulted in the fastest reaction rate, Fig. 2. This

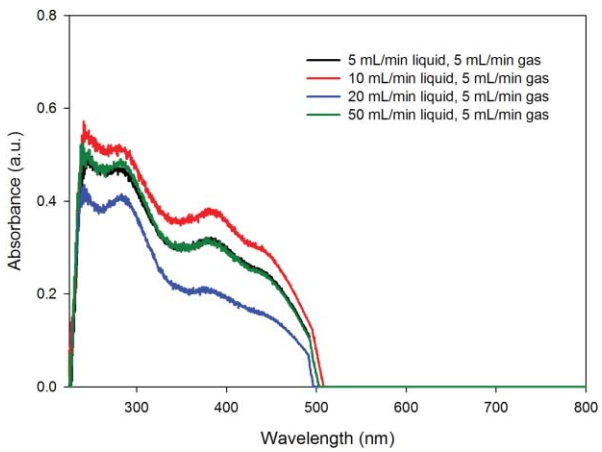

Fig. 2 Comparison of UV-Vis absorption intensity using different flow parameters for 0.05% w/v NaPP at 70 °C after 10 minutes.

observation is valid since the measured particle size distributions are similar for all flow rates, and therefore the extinction coefficient of the colloidal solutions are similar. When compared with a batch experiment using the same reagent volume and hydrogen flow rate, the optimal NCR flow conditions also yielded a faster reaction. This is most likely due to optimal gas–liquid mass transfer, and therefore more rapid saturation of the solution with hydrogen under these flow conditions. Gas–liquid mass transfer occurs across the thin film of liquid between the gas slug and the tube wall, rather than at the interface between the gas and liquid slugs. It has been previously shown that gas–liquid mass transfer is enhanced in a Taylor flow system compared to stirred batch reactors, with the rate of mass transfer dependent on the length of the liquid and gas slugs.[22]

As the reagent volume increases, however, for the same flow rate the batch reaction becomes quicker since a smaller fraction of the solution has been exposed to NCR conditions (see ESI†). For example, after 30 minutes at a liquid flow rate of 10 mL min^{-1}, a 200 mL volume of feed solution would have passed through the recirculating NCR 1.5 times, whereas a 50 mL feed solution would have passed through 6 times and a 2 L feed solution would have passed through 0.15 times. Since only a fraction of the 2 L reagent feed solution has been exposed to hydrogen and NCR conditions after 30 minutes, the batch bubbling experiment yielded a faster reaction rate, simply due to all of the solution being exposed to hydrogen. Upon inspection of the optical properties of the product from the recirculating NCR for a 2 L volume of feed solution after any time, it was observed the peak silver plasmon intensity is unexpectedly high when compared to that for smaller volumes of feed solution. This is a consequence of a flaw in the design of the recirculating NCR, whereby the reduction reaction continues to occur outside the NCR in the feed solution, which is equivalent to a stirred batch reactor.

The reactions were continued until no noticeable change was observed in the UV-Vis absorption spectra (approximately 2 hours). At this concentration of NaPP the nanoparticle size distribution is rather large, with nanoparticles ranging in size from 2 nm to in excess of 20 nm in diameter. The average particle size from the optimal flow conditions after 2 hours was 6.4 ± 4.2 nm, Fig. 3. The plasmon absorption band is very wide, Fig. 2, and this has been ascribed to the presence of sub-nanometre silver nanoclusters.[10] The absence of anisotropic silver nanoparticles, such as nanorods, that could also create such optical absorption properties, indicates that nanoclusters, which are too small to observe using TEM, may be present.

Increasing the NaPP concentration and modifications to the flow regime did not produce more monodisperse particles, but decreases in the NaPP concentration and the reaction temperature both led to a decrease in particles size and the formation of more monodisperse particles. When the concentration of NaPP was reduced to 0.01% w/v the average particle size decreased to 4.4 ± 1.8 nm, but this is associated with a decrease in reaction rate, which was evident by the longer time required for any change in the UV-Vis absorption spectrum to be observed. The optical properties of the colloidal silver solutions change with NaPP concentration, with the silver plasmon absorption band becoming narrower as the concentration of NaPP decreases, Fig. 4, and when the concentration is too low, little reaction takes place.

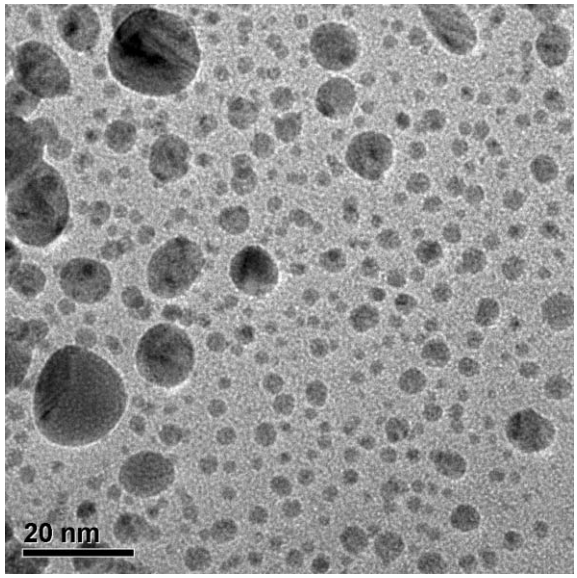

Fig. 3 TEM image of Ag nanoparticles produced at optimised flow conditions with 0.05% w/v NaPP at 70 °C after 120 minutes.

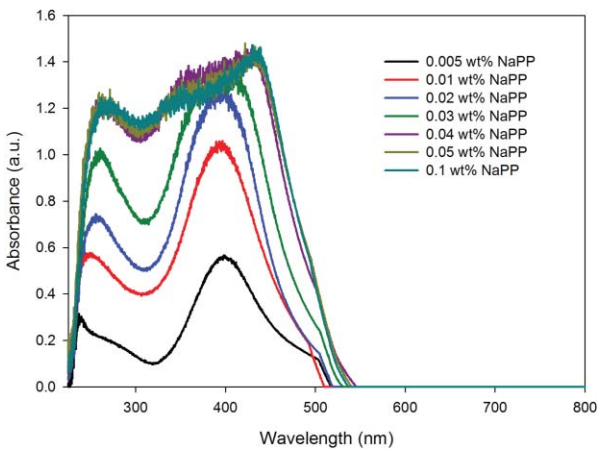

Fig. 4 Comparison of UV-Vis absorption intensity with different NaPP concentrations at 70 °C after 120 minutes.

Comparison of the particle size and polydispersity between batch and recirculating NCR reactions revealed little difference between the products obtained from both techniques. This is again a consequence of a design flaw in the recirculating NCR, that being the reduction reaction can take place outside the NCR in the reagent feed solution. The output solution contains unreacted hydrogen which can react with silver ions in the reagent feed solution, and therefore a batch reaction also occurs in the recirculating NCR setup. Since the reaction requires an elevated temperature to occur at an appreciable rate, it is possible to prevent or minimise the reaction that occurs in the reagent feed solution by not heating this feed. A decrease of the reactor temperature and the reagent feed solution to 40 °C resulted in a substantial decrease in the average particle diameter, with the final particles at 3.1 ± 1.2 nm, but this was associated with a substantial decrease in reaction rate, with the subsequent reaction requiring 4 hours to complete. Interestingly, however, the reaction could be modified with the reagent feed heated to 40 °C, and the NCR heated to 70 °C, resulting in an increase in

reaction rate with no influence on the final particle size, Fig. 5. At low temperatures the reaction does not proceed rapidly, and therefore a design feature where the reagent feed solution is kept relatively cool compared to the NCR will minimise the amount of reduction that occurs in what can be described as the stirred-batch reactor component of the NCR design. Under these conditions, the reaction in the recirculating NCR took place much quicker than a batch reaction at 40 °C, but this may be due not only to greater mass transfer but also due to the fluid being temporarily heated in the recirculating NCR.

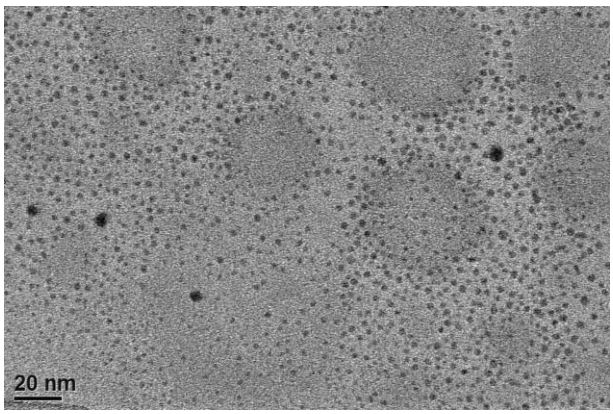

Fig. 5 TEM image of small silver nanoparticles produced at 40 °C feed temperature, 70 °C NCR temperature with 0.05% w/v NaPP.

Influence of polyphosphate type

In the presence of 0.05% w/v NaTPP at 70 °C, using the optimised flow parameters for NaPP, a much faster reaction was evident, but the size of the particles (36 ± 19 nm) were more polydispersed than for reactions in the presence of NaPP. The optical properties of these colloidal solutions are slightly different to those produced with NaPP. A narrower silver plasmon absorption in the presence of NaTPP may be indicative of the lack of formation of sub-nanometre silver nanocluster species, which is most likely due to the shorter chain length of NaTPP. It is possible that some Ag^{+} and Ag^{0} species bound to NaPP are protected from growth more than the silver species bound to the NaTPP chain, since the chain length of NaPP is 4 times longer than that of NaTPP, but studies on the morphology of the polyphosphates and the silver–polyphosphate complexes in solution at different temperatures and pH levels are required to determine the cause of the differences observed. A comparison of the evolution of the optical properties of these colloidal solutions is provided in the ESI.† Again, a decrease in NaTPP concentration and reaction temperature resulted in smaller and more monodisperse particles. At 0.01% w/v the average particle size was found to be 5.2 ± 1.9 nm, and at 0.005% w/v the particle size was 2.6 ± 0.9 nm, at a feed temperature of 40 °C and an NCR temperature of 70 °C, Fig. 6. Since the reaction with NaTPP is much faster than that with NaPP, a lower concentration of NaTPP can be used, such as 0.005% w/v, without observing a substantially smaller extent of reaction (see ESI†). The particles produced with either NaPP or NaTPP using a low temperature method were stable for at least one year.

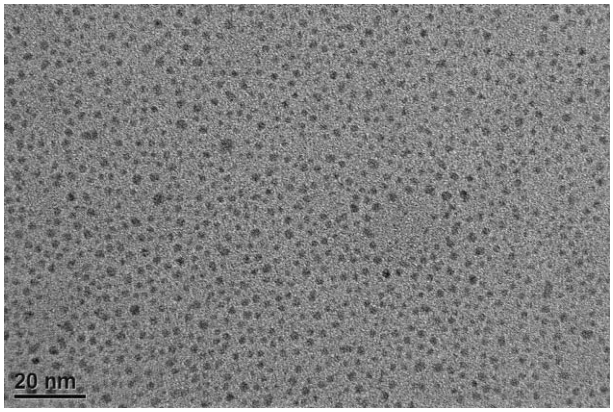

Fig. 6 TEM image of small silver nanoparticles produced with 0.005% w/v NaTPP at 40 °C feed temperature, 70 °C NCR temperature.

The results presented for the recirculating NCR show that there is little influence of flow rate on the size and polydispersity of the silver nanoparticles produced. Only the rate of reaction is influenced by change in flow rate and this is also dependent on the volume of the reagent feed solution. The size and polydispersity is mainly dependent on the concentration of polyphosphate and the temperature of the NCR and the reagent feed solution, since a significant amount of reaction appears to occur in the stirred batch reactor part of the recirculating NCR. In order to determine the influence of segmented gas–liquid flow on the size and polydispersity of the nanoparticles produced, as well as accessing the synthesis with extremely low polyphosphate concentrations, a different NCR design was necessary.

Pressurised, high-temperature, single-pass NCR

The reason for the construction of a long-path-length, pressurised, high-temperature, single-pass NCR was to overcome the limitations of the recirculating NCR, namely the very long reaction times and backmixing of the colloid solution which provides seed particles on which additional silver metal can grow, thereby increasing particle size and polydispersity. Using the conditions developed for generating small silver nanoparticles of relatively low polydispersity using a recirculating NCR, *i.e.*, low polyphosphate concentrations, the influence of temperature and flow conditions was investigated. If the NCR was heated above 120 °C, and if the total flow rate of liquid and gas was less than 5 mL min^{-1}, that a significant amount of silver was deposited on the inner wall of the NCR. In contrast, if the total flow rate of gas and liquid was greater than 10 mL min^{-1}, significantly less reaction occurred. The optimum flow rate was 5 mL min^{-1} for both the gas and the liquid feeds, at a reactor temperature of 120 °C. In order for the liquid to be heated to this temperature, the reactor must be pressurised to a pressure equal or greater than the vapour pressure of water at 120 °C, and this has been achieved with a back-pressure regulator. The vapour pressure of water at 120 °C is 198.67 kPa (28.8 psi) and the pressure of the reactor was set to 206.8 kPa (30 psi). It should be noted that the gas flow rates are measured in sccm (standard cubic centimetres per minute), and therefore when the reactor is pressurised to 30 psi, the gas flow is reduced from 5 mL min^{-1} (sccm) to 1.64 mL min^{-1}. Another advantage of a

pressurised system is the increase in hydrogen solubility, which can be approximated using Henry's law. Since more hydrogen will be available in solution at higher pressures (but less would be available at higher temperatures), enhanced reaction kinetics are likely to be observed. Using a temperature-dependent expression of Henry's law, eqn (1), the solubility of hydrogen in solution can be approximated, where k_H^0 is the Henry's law constant at standard temperature, C is a constant pertaining to a specific gas (500 K for H_2), and T and T^0 are the absolute temperature of the system and absolute standard temperature, respectively.[23]

$$k_H = k_H^0 \exp\left[-C\left(\frac{1}{T} - \frac{1}{T^0}\right)\right] \quad (1)$$

At 120 °C and 30 psi (44.7 psi total) the hydrogen solubility is approximately 9.32×10^{-4} M, whilst for the 70 °C reaction at ambient pressure in the recirculating NCR, the hydrogen solubility is 3.3×10^{-4} M. These values are only approximations since Henry's law assumes that the gas is not reactive with the solution.

In this single-pass NCR setup the amount of polyphosphate that can be used is significantly less than that for the recirculating NCR, whilst still achieving similar absorption intensities, *i.e.*, the production of Ag nanoparticles with a similar concentration, due to the higher reaction temperature that can be utilised. Given the results from the recirculating NCR, this means that small nanoparticles would likely be obtained more rapidly in the single-pass setup. Fig. 7 shows a TEM image of 3.5 ± 0.9 nm silver nanoparticles produced with 0.0025% w/v NaPP at 120 °C along with the corresponding absorption spectrum. This method has a clear advantage over the low temperature route since the time required for this reaction to occur, *i.e.*, the fluid residence time under these flow conditions, is approximately only 9.1 minutes. As the concentration of NaPP is increased the nanoparticle size increases with increasing polydispersity, affording similar results to that obtained with the recirculating reactor. Applying the same reaction temperature used in the recirculating reactor, *i.e.*, 70 °C, in the one-pass reactor, with 0.05% w/v NaPP and without pressurising the reactor, gives similar results to that obtained with the recirculating NCR and batch reactions, indicating that superior mixing conditions in the one-pass reactor under plug flow conditions do not influence the final size of the silver nanoparticles. Reactions with 0.05% w/v NaTPP at 70 °C were attempted in the single-pass NCR and it was found that there is an improvement in the polydispersity of the final product. The particle size approaches that obtained using NaPP, 10.2 ± 5.8 nm, but the reasons for this improvement and why this improvement is only seen for NaTPP are unclear. Since the reaction is much faster using NaTPP, a significantly greater portion of the reaction may have occurred in the stirred batch portion of the recirculating NCR with NaTPP than with NaPP. The particle size obtained, however, is still inferior to that obtained at lower temperatures and lower polyphosphate concentrations. Reactions at 40 °C at a pressure of 30 psi were attempted for various polyphosphate concentrations, but little reaction was observed for all concentrations, indicating that although the hydrogen solubility has significantly increased (1.4×10^{-3} M), temperature is also a critical parameter determining reaction kinetics.

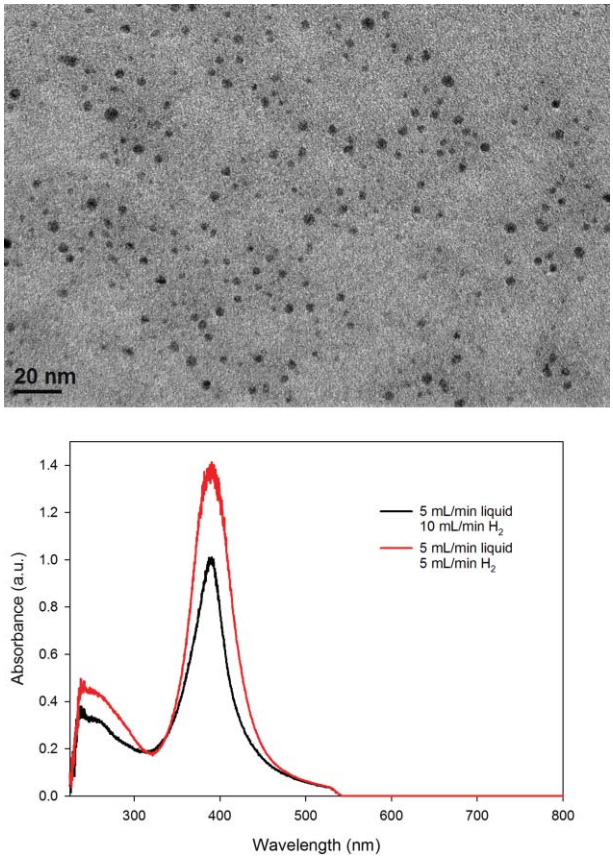

Fig. 7 Top: TEM image of silver nanoparticles produced with 0.0025% w/v NaPP at 120 °C at 5 mL min^{-1} liquid and gas. Bottom: UV-Vis absorption spectra for 0.0025% w/v NaPP at 120 °C at different flow conditions.

Conclusions

Batch and process intensification methodologies have been explored for the continuous flow synthesis of very small silver nanoparticles. Small silver particles, 3–5 nm in diameter, are produced at low concentrations and low temperatures using batch processing and a recirculating NCR design. The pressurised, high-temperature, single-pass NCR enables the effective use of much less NaPP and NaTPP, and produces small silver nanoparticles at high temperature and low polyphosphate concentrations. In comparison to the previously published synthesis of small silver nanoparticles with hydrogen in the presence of phosphonated calixarenes, similar quality nanoparticles can be produced without the need for a multi-step and energy intensive synthesis of the calixarene, thus providing a greener synthesis method in accessing small silver nanoparticles. The use of sodium tripolyphosphate allows for a more rapid synthesis of silver nanoparticles than with sodium polyphosphate, and a lower quantity of the tripolyphosphate can be used at lower reaction temperatures without restricting the reaction rate. Further work is planned to apply this synthesis to other precious metal systems. The use of significantly greater hydrogen pressures to enhance reaction kinetics is also being considered, in

both a recirculating and single-pass NCR, as well as application of the reaction to a microfluidic chip. A design whereby unused hydrogen can be recycled into the reactor is another feature currently under consideration so that the efficiency of the overall production is improved.

Acknowledgements

The authors acknowledge the facilities, scientific and technical assistance of the Australian Microscopy & Microanalysis Research Facility at the Centre for Microscopy, Characterisation & Analysis, The University of Western Australia, a facility funded by The University, State and Commonwealth Governments. The authors would also like to acknowledge financial support from the New York State Office of Science, Technology and Academic Research (NYSTAR) and the Australian Research Council (ARC), as well as technical assistance from Srinivasan Ambatipati. KJH would like to acknowledge the Australian-American Fulbright Commission and BHP Billiton for the award of a Fulbright Scholarship in Science and Engineering and a Hackett Scholarship from The University of Western Australia.

Notes and references

1 C. C. Baker, A. Pradhan and S. I. Shah, *Encyclopedia of Nanoscience and Nanotechnology*, 2004, **5**, 449–473.
2 J. Turkevich, P. C. Stevenson and J. Hillier, *Discuss. Faraday Soc.*, 1951, **11**, 55–75.
3 M. Giersig and P. Mulvaney, *Langmuir*, 1993, **9**, 3408–3413.
4 G. Frens, *Nature Physical Science*, 1973, **241**, 20–22.
5 P. Raveendran, J. Fu and S. Wallen, *J. Am. Chem. Soc.*, 2003, **125**, 13940–13941.
6 P. Raveendran, J. Fu and S. L. Wallen, *Green Chem.*, 2006, **8**, 34–38.
7 D. D. Evanoff and G. Chumanov, *ChemPhysChem*, 2005, **6**, 1221–1231.
8 K. S. Iyer, C. L. Raston and M. Saunders, *Lab Chip*, 2007, **7**, 1800–1805.
9 K. J. Hartlieb, M. Saunders and C. L. Raston, *Chem. Commun.*, 2009, 3074–3076.
10 B. Ershov and E. Abkhalimov, *Colloid J.*, 2007, **69**, 579–584.
11 T. Linnert, P. Mulvaney, A. Henglein and H. Weller, *J. Am. Chem. Soc.*, 1990, **112**, 4657–4664.
12 P. Mulvaney and A. Henglein, *J. Phys. Chem.*, 1990, **94**, 4182–4188.
13 B. G. Ershov and A. Henglein, *J. Phys. Chem. B*, 1998, **102**, 10663–10666.
14 D. Evanoff and G. Chumanov, *J. Phys. Chem. B*, 2004, **108**, 13948–13956.
15 D. Evanoff and G. Chumanov, *J. Phys. Chem. B*, 2004, **108**, 13957–13962.
16 R. Jachuck, G. Pherwani and S. M. Gorton, *J. Environ. Monit.*, 2009, **11**, 642–647.
17 R. J. J. Jachuck, D. K. Selvaraj and R. S. Varma, *Green Chem.*, 2006, **8**, 29–33.
18 E. McCarthy, W. Dunk and K. Boodhoo, *J. Colloid Interface Sci.*, 2007, **305**, 72–87.
19 V. S. Shirure, B. P. Nikhade and V. G. Pangarkar, *Ind. Eng. Chem. Res.*, 2007, **46**, 3086–3094.
20 V. S. Shirure, A. S. Pore and V. G. Pangarkar, *Ind. Eng. Chem. Res.*, 2005, **44**, 5500–5507.
21 G. Trippa and R. Jachuck, *Chem. Eng. Res. Des.*, 2003, **81**, 766–772.
22 J. J. Heiszwolf, M. T. Kreutzer, M. G. van den Eijnden, F. Kapteijn and J. A. Moulijn, *Catal. Today*, 2001, **69**, 51–55.
23 D. Lide and H. P. R. Frederikse, eds, *CRC Handbook of Chemistry and Physics*, CRC Press, Inc., Boca Raton, FL, 76th edn, 1995.